

# Gene editing in human stem cells using zinc finger nucleases and integrase-defective lentiviral vector delivery

Angelo Lombardo<sup>1,2</sup>, Pietro Genovese<sup>1,2</sup>, Christian M Beausejour<sup>3,6</sup>, Silvia Colleoni<sup>4</sup>, Ya-Li Lee<sup>3</sup>, Kenneth A Kim<sup>3</sup>, Dale Ando<sup>3</sup>, Fyodor D Urnov<sup>3</sup>, Cesare Galli<sup>4,5</sup>, Philip D Gregory<sup>3,7</sup>, Michael C Holmes<sup>3,7</sup> & Luigi Naldini<sup>1,2,7</sup>

**Achieving the full potential of zinc-finger nucleases (ZFNs) for genome engineering in human cells requires their efficient delivery to the relevant cell types. Here we exploited the infectivity of integrase-defective lentiviral vectors (IDLV) to express ZFNs and provide the template DNA for gene correction in different cell types. IDLV-mediated delivery supported high rates (13–39%) of editing at the IL-2 receptor common  $\gamma$ -chain gene (*IL2RG*) across different cell types. IDLVs also mediated site-specific gene addition by a process that required ZFN cleavage and homologous template DNA, thus establishing a platform that can target the insertion of transgenes into a predetermined genomic site. Using IDLV delivery and ZFNs targeting distinct loci, we observed high levels of gene addition (up to 50%) in a panel of human cell lines, as well as human embryonic stem cells (5%), allowing rapid, selection-free isolation of clonogenic cells with the desired genetic modification.**

Site-specific manipulation of the genome has revolutionized biology and holds promise for molecular medicine<sup>1</sup>. The homologous recombination pathway, which evolved to resolve stalled DNA replication forks, repair DNA double-strand (ds) breaks and foster genetic recombination<sup>2</sup>, can be exploited to edit a specific locus. After delivery of DNA molecules that are largely identical in sequence to the target locus but contain mismatches or intervening sequences, homologous recombination mediates incorporation of the novel sequence into a small fraction of the treated cells<sup>3,4</sup>. If selector genes are included in the donor sequence, the genetically modified cells can be isolated. Despite being labor intensive, this approach allows knocking-in and knocking-out of genes in rodent embryonic stem (ES) cells and generation of transgenic lines, which are invaluable for discovering gene function<sup>1,5,6</sup>, technology recently recognized by the Nobel Committee.

It has long been envisaged that by applying a similar strategy to patient-derived stem cells, inherited mutations could be repaired and corrected cells generated to repopulate the affected tissues and reverse the disease<sup>7</sup>. Gene correction overcomes the major limitations of gene-replacement strategies, as it restores both the function and expression control of the affected gene and avoids the risks associated with semi-random vector integration<sup>8–11</sup>. Indeed, whereas retroviral vector-mediated gene transfer into hematopoietic stem cells has conferred therapeutic benefit in severe combined immunodeficiencies (SCID)<sup>12–15</sup>, some treated X-linked SCID patients developed leukemia. Transformed cell growth was consequent to oncogene activation at the site of vector integration<sup>16</sup> and may have been facilitated by deregulated expression of the IL-2 receptor common  $\gamma$ -chain (*IL2RG*) therapeutic transgene<sup>17,18</sup>. Thus, the safety of gene therapy would be improved by targeting vector integration to specific genomic sites or by developing more effective gene correction strategies<sup>3,4,19–23</sup>.

Recently, ZFNs have been used to enhance the frequency of gene correction<sup>24–26</sup>. In this approach, the C<sub>2</sub>H<sub>2</sub> class of zinc-finger DNA-binding domains<sup>27</sup> is engineered to recognize a DNA sequence of interest<sup>28,29</sup> and fused to the nuclease domain of the *FokI* endonuclease to yield a highly specific ZFN<sup>30</sup>. Because *FokI* must dimerize to induce a ds break<sup>31</sup>, two different ZFNs are designed that bind to the sequence of interest in the opposite orientation and with the correct spacing. A ZFN-induced ds break in the chromosome is repaired by nonhomologous end joining (NHEJ), an error-prone process that can lead to disruption of the targeted gene, or by homology-directed repair (HDR), a form of homologous recombination that faithfully copies the genetic information from a DNA molecule of related sequence<sup>32</sup>. Using ZFNs designed against the human *IL2RG* locus and a donor DNA sequence containing a silent point mutation, we have reported efficient conversion of the endogenous sequence into the donor-encoded one in cell lines<sup>33</sup>. However,

Recently, ZFNs have been used to enhance the frequency of gene correction<sup>24–26</sup>. In this approach, the C<sub>2</sub>H<sub>2</sub> class of zinc-finger DNA-binding domains<sup>27</sup> is engineered to recognize a DNA sequence of interest<sup>28,29</sup> and fused to the nuclease domain of the *FokI* endonuclease to yield a highly specific ZFN<sup>30</sup>. Because *FokI* must dimerize to induce a ds break<sup>31</sup>, two different ZFNs are designed that bind to the sequence of interest in the opposite orientation and with the correct spacing. A ZFN-induced ds break in the chromosome is repaired by nonhomologous end joining (NHEJ), an error-prone process that can lead to disruption of the targeted gene, or by homology-directed repair (HDR), a form of homologous recombination that faithfully copies the genetic information from a DNA molecule of related sequence<sup>32</sup>. Using ZFNs designed against the human *IL2RG* locus and a donor DNA sequence containing a silent point mutation, we have reported efficient conversion of the endogenous sequence into the donor-encoded one in cell lines<sup>33</sup>. However,

<sup>1</sup>San Raffaele Telethon Institute for Gene Therapy and <sup>2</sup>"Vita Salute San Raffaele" University, via Olgettina, 58, 20132 Milan, Italy. <sup>3</sup>Sangamo BioSciences, Inc., Pt. Richmond Tech Center, 501 Canal Blvd., Suite A100 Richmond, California 94804, USA. <sup>4</sup>Reproductive Technologies Laboratory, CIZ, Istituto Sperimentale Italiano Lazzaro Spallanzani, via Porcellasco 7/F, 26100 Cremona, Italy. <sup>5</sup>Dipartimento Clinico Veterinario, University of Bologna, Via Tolara di Sopra 50, 40064 Ozzano Emilia, Italy. <sup>6</sup>Present address: Département de Pharmacologie, Centre de Recherche, CHU Ste-Justine 3175, Côte Ste-Catherine, Montréal, Quebec H3T 1C5, Canada. <sup>7</sup>These authors contributed equally to this work. Correspondence should be addressed to L.N. (naldini.luigi@hsr.it).

Received 21 March; accepted 9 October; published online 28 October 2007; doi:10.1038/nbt1353

codelivery of two ZFNs and the donor DNA in primary cells represents a major hurdle for the exploitation of ZFN-mediated genetic manipulation of primary cells. Here we describe a gene delivery approach based on IDLV<sup>34–38</sup> that allows gene editing and targeted transgene addition in most cell types, including human primary hematopoietic stem cells and ES cells.

## RESULTS

### ZFN-mediated editing of an endogenous gene by IDLV delivery

Previous studies showed that HIV vectors packaged with the D64V integrase mutant (IDLV) are competent for infection and nuclear delivery of vector DNA but completely defective for integrase-mediated integration<sup>34–39</sup>. In IDLV-transduced cells, vector DNA is found as both linear and 1-, 2-long terminal repeat (LTR) circular episomes that are progressively lost upon cell proliferation. Consistent with the short-term vector persistence, infected cells demonstrate a transient wave of transgene expression (Supplementary Fig. 1 online).

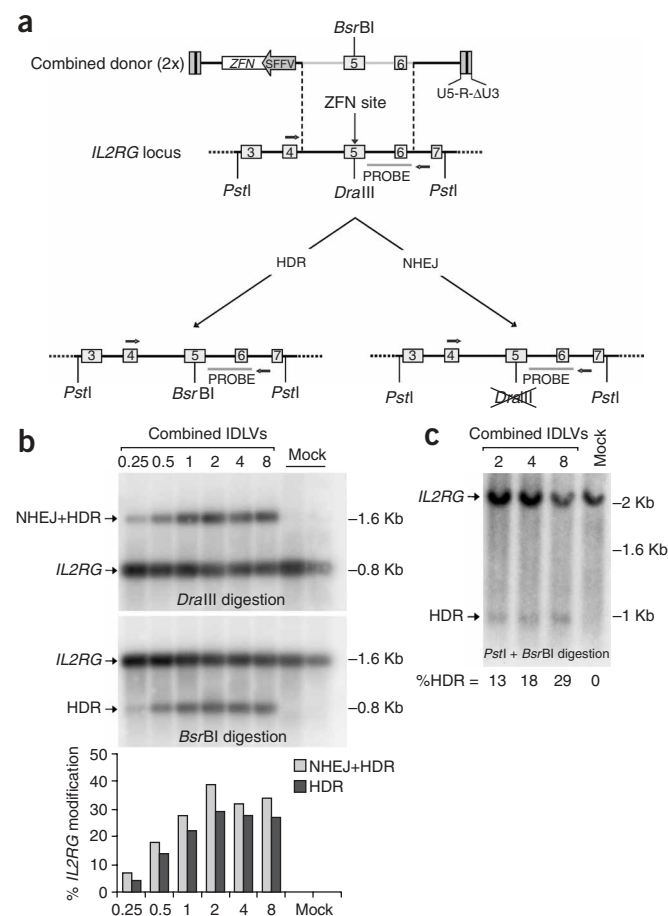
To determine whether IDLV delivery of ZFNs and donor DNA can mediate gene correction, we used a human embryonic kidney (HEK) 293 reporter cell line that carries the gene encoding green fluorescent protein (*GFP*), whose expression is disabled by insertion of a sequence from the *IL2RG* exon 5 (ref. 33). ZFNs targeting the *IL2RG* sequence can induce a ds break in the defective *GFP* gene and trigger its HDR if a suitable donor sequence is available. We cotransduced the cells with three different IDLVs, two of them expressing the ZFNs and a third containing the donor sequence, and showed that IDLVs can drive ZFN expression levels sufficient for stimulating gene correction and are proficient substrates for HDR (Supplementary Fig. 2 online). As expected, IDLV-induced ZFN activity in transduced cells was transient, detectable only for the first 3–4 d after infection (Supplementary Fig. 3 online).

**Figure 1** Editing of the endogenous *IL2RG* gene by IDLV delivery of ZFNs and donor DNA. **(a)** Top: schematic of a combined lentiviral vector containing donor sequences homologous to *IL2RG* (gray line, boxes indicate exons) and a ZFN expression cassette. Two such vectors are used to express the *IL2RG* ZFN pair (2×). The product of reverse transcription of the vector is depicted and the constituent regions of the 5' self-inactivating LTR are indicated ( $\Delta U3$ -R-U5). The donor DNA contains a silent point-mutation that is copied into *IL2RG* exon 5 via ZFN-mediated HDR inserting a new *Bsr*BI restriction site. Middle: schematic of the *IL2RG* locus; note the *Dra*III restriction site within the ZFN target site in exon 5. Bottom: schematics of the *IL2RG* locus upon gene conversion (HDR) or NHEJ. The positions of the PCR primers (black arrows), restriction sites and probe used for analyses are indicated. SFFV, spleen focus forming virus LTR promoter. **(b)** K-562 cells were infected with the indicated doses ( $\mu$ g HIV-1 Gag p24/ml) of two IDLVs expressing either *IL2RG*-targeting ZFN and analyzed 15 d post-transduction by semiquantitative PCR amplifying the *IL2RG* locus from primers external to the donor homology. PCR amplicons were digested as indicated and visualized by Southern blot (see schematic in **a** for the location of primers (arrows), restriction sites and probe sequence). Elimination of a chromosomal *Dra*III site within the ZFN recognition sequence indicates editing of the locus by either NHEJ or HDR (NHEJ+HDR, upper blot, 1.6-Kb band), whereas exchange of the *Dra*III site with the donor-encoded *Bsr*BI site indicates gene conversion via HDR (lower blot, 0.8-Kb band). The histogram shows the percentage of each modification at the *IL2RG* locus calculated by densitometric scanning of the blots. Data shown are representative of three independent experiments. **(c)** Southern blot of genomic DNA digested with the indicated restriction enzymes 1 month post-transduction confirmed gene conversion (see schematic in **a** for the location of the restriction sites and probe sequence). The percentage of HDR calculated by densitometric scanning is shown at the bottom.

To assess gene conversion at the endogenous *IL2RG* locus, we used a donor sequence containing a silent point mutation that inserts a novel restriction site within exon 5 of the gene. We combined the donor sequence and a ZFN expression cassette in the same vector (Fig. 1a) and treated human hematopoietic K-562 cells with increasing doses of the two IDLVs. Using semiquantitative PCR followed by digestion with two different restriction enzymes (Fig. 1b), we measured up to 39% *IL2RG* editing, with gene conversion accounting for 74% of all events ( $16 \pm 9\%$ , mean  $\pm$  s.d. gene conversion,  $n = 14$ ). Gene conversion was confirmed by Southern blot analysis (Fig. 1c).

We then transduced Epstein-Barr virus-transformed B lymphocytes (lymphoblastoid cells) from a normal male donor with the IDLVs described in Figure 1a and found up to 13% *IL2RG* editing, with gene conversion accounting for 61% of all events ( $5 \pm 1.5\%$ , mean  $\pm$  s.d. gene conversion,  $n = 7$ ; Fig. 2a). *IL2RG* genotype (Fig. 2b) and  $\gamma$ -chain expression (Fig. 2c) analysis of 64 clones randomly isolated from the treated cells showed gene disruption in three clones and gene conversion in two clones. In the latter clones,  $\gamma$ -chain expression was maintained at a normal level. There was no significant difference in the percentage of gene editing between the clones and the bulk culture (by Fisher's exact test). ZFN-mediated gene editing was confirmed by sequencing of the PCR products (data not shown). None of the edited clones contained integrated vector, as assessed by PCR (data not shown).

These results show that IDLV delivery of ZFNs and donor DNA sequence induces efficient gene editing in multiple human cell types, making possible direct monitoring of bulk unselected cell populations and rapid isolation of clones bearing the desired genotype.



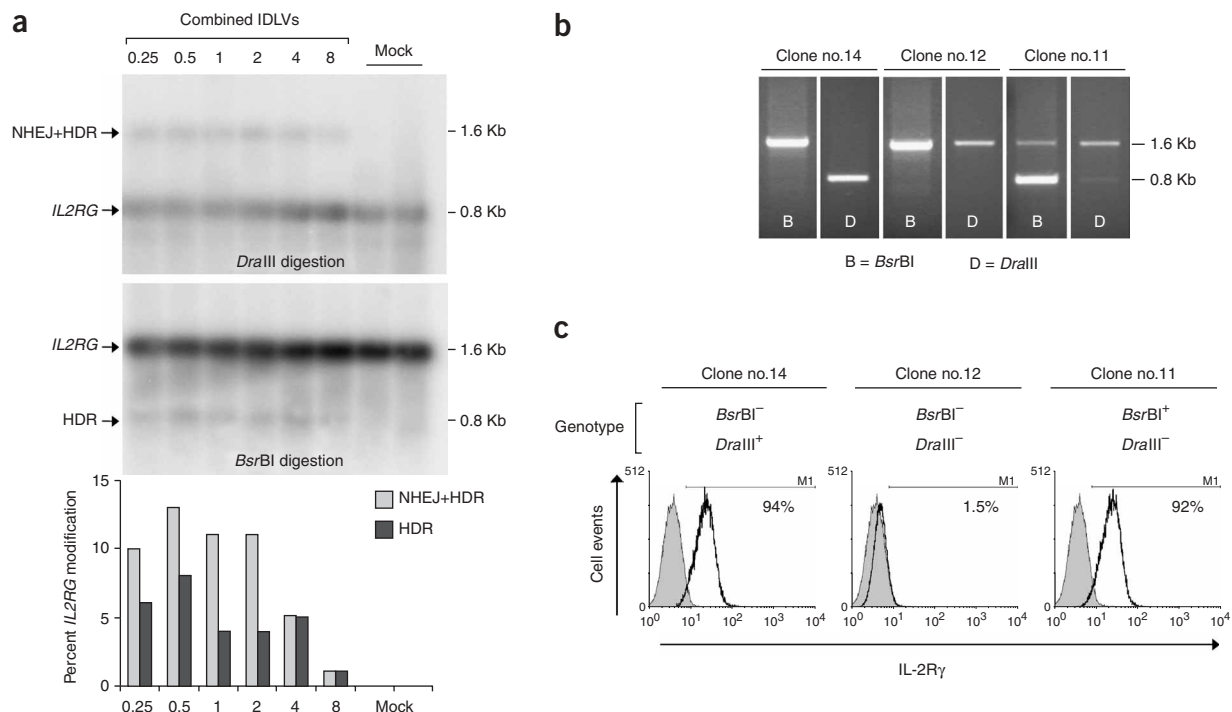


**Figure 2** *IL2RG* gene editing in human lymphoblastoid cells. **(a)** Cells from a normal male donor were treated with the indicated doses of combined IDLVs, and editing at *IL2RG* was analyzed 15 d after transduction (**Fig. 1b**). The histogram shows the percentage of each modification (NHEJ+HDR or HDR alone) at the *IL2RG* locus. **(b)** Randomly selected clones were isolated by limiting dilution from the 0.5  $\mu$ g p24/ml IDLV-treated cells in **a**, and genotyped by PCR and restriction enzyme digestion. Clone no. 14 shows a wild-type genotype, whereas clones no. 12 and no. 11 show digestion patterns indicative of gene disruption (NHEJ; *DraIII* resistance) or conversion (HDR, *BsrBI* sensitivity and *DraIII* resistance), respectively. **(c)** Expression of the IL-2R $\gamma$  measured by FACS in clones genotyped in **b**. Clones no. 12 and no. 11 show expression consistent with their genotypes, namely, loss of  $\gamma$ -chain expression and normal expression, respectively. The genotype of the clones is indicated on top of the histograms. Filled histograms represent the isotype controls. Data shown are representative of three independent experiments.

### ZFN-mediated targeted transgene addition into the *IL2RG* gene

Because proximity of the mutation to the ZFN cleavage site is necessary for gene correction<sup>40</sup>, each cluster of X-SCID-causing mutations<sup>41</sup> would require ZFNs tailored to that site. In the HEK293-based gene correction system, we found that a reporter cassette flanked on both sides by sequences homologous to the target locus became integrated into the ZFN target site in 15% of the corrected cells (**Supplementary Fig. 4** online). This raised the possibility of using a single pair of ZFNs to knock-in an *IL2RG* cDNA that could restore wild-type function to a broad spectrum of X-SCID genotypes.

To test this approach, we placed a *GFP* expression cassette within the *IL2RG* homology arms of the donor vector (**Fig. 3a**) and treated K-562 cells with this donor-IDLV, either alone or together with increasing doses of the two *IL2RG* ZFN-expressing IDLVs. The percentage of GFP<sup>+</sup> cells increased as the doses of the ZFN-expressing IDLVs increased, reaching up to 6.3% (3.4  $\pm$  1%, mean  $\pm$  s.d.,  $n = 9$ ), whereas it was 1.1% in cells treated with donor-IDLV alone (**Fig. 3b**). PCR analysis on GFP<sup>+</sup> cells sorted by fluorescence-activated cell sorting (FACS) showed the expected integration junctions between the *GFP* cassette and the *IL2RG* locus in cells treated with donor- and ZFN-IDLVs (**Fig. 3c**). Southern blot and PCR analyses performed on the sorted cells and on a panel of clones randomly isolated from them (**Fig. 3d** and **Supplementary Fig. 5** online) showed that the vast majority of the integrated *GFP* cassette was found at the *IL2RG* ZFN target site, either as a single expression cassette or in the form of a head-to-tail concatemer with intervening vector sequences. The

mechanism of integration was consistent with HDR of the ZFN target site. When the same targeting strategy was used to treat human lymphoblastoid cells, we found up to 2.4% GFP<sup>+</sup> cells after donor- and ZFN-IDLVs treatment (1.8  $\pm$  0.7% mean  $\pm$  s.d.,  $n = 9$ ; **Fig. 4a**) versus 0.2% GFP<sup>+</sup> cells in the donor-IDLV-alone condition. As expected from the insertion of the *GFP* cassette into the single *IL2RG* locus of male cells (**Fig. 4b**),  $\gamma$ -chain expression was lost in the GFP<sup>+</sup> cells (**Fig. 4c**). These experiments showed that codelivery of donor- and ZFN-IDLVs resulted in the targeted addition of an expression cassette into the genomic ZFN target site with high efficiency and specificity.

We then constructed a donor vector carrying a promoterless 0.8-kb stretch of the *IL2RG* cDNA (**Fig. 4d**) that encoded the wild-type protein C-terminal to proline 229. We treated lymphoblastoid cells with donor- and ZFN-IDLVs and found addition of the donor-encoded cDNA in up to 6% of the *IL2RG* alleles, which corresponds to 6% of these genotypically male cells (**Fig. 4e**). Expression of the integrated construct was verified by RT-PCR using primers specific for silent mutations introduced into the donor-encoded sequence (**Fig. 4f**). Because the donor construct lacks a promoter and integration is targeted to the *IL2RG* ZFN site, expression of the donor-encoded cDNA reflects the activity of the endogenous *IL2RG* promoter.

These data show that a system combining IDLV delivery and ZFN-mediated gene targeting (IDLV-ZFN) can specifically integrate into the *IL2RG* locus an open reading frame that would reconstitute physiological expression of  $\gamma$ -chain in carriers of mutations within and downstream of exon 5.

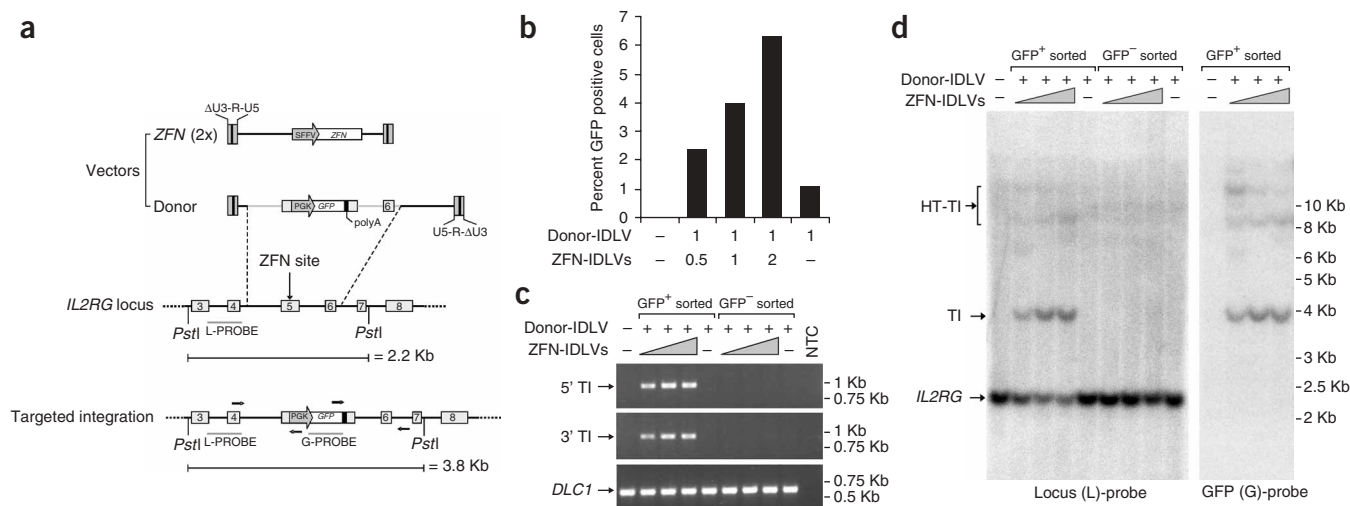


**Figure 3** Targeted transgene addition into *IL2RG*. **(a)** Top: schematic of the ZFN-expressing vectors and the donor vector containing homology sequences to the *IL2RG* gene (gray lines, boxes indicate exons) flanking a PGK-*GFP* expression cassette. PGK, phosphoglycerate kinase gene promoter. Middle: schematic of the endogenous locus showing the ZFN target site. Bottom: schematic of the result of targeted addition of the PGK-*GFP* cassette into the *IL2RG* locus mediated by HDR. The expected fragments from *Pst*I digest, PCR primers (black arrows) and the probes used in the analysis are indicated. **(b)** K-562 cells were treated with the indicated IDLV doses and analyzed by FACS for GFP expression 1 month after transduction. Data are representative of three independent experiments. **(c)** The treated cells were sorted according to GFP expression and analyzed by PCR for targeted integration (TI) into the ZFN site in the *IL2RG* locus using two sets of primers specific for the 5' or 3' integration junctions. The bottom gel shows control amplification from a nontargeted locus (8p22; *DLC1* gene). NTC: no template control. **(d)** Southern blot analysis of genomic DNA from the sorted cells in **c** using a locus probe (L; sequence outside of the homology region included in the vector) and, after stripping of the membrane, a *GFP* probe (G). Targeted integration of the cassette at the *IL2RG* locus (TI) was observed in the GFP<sup>+</sup> cells co-treated with donor- and ZFN-IDLVs, but not in cells treated with donor-IDLV only. Higher molecular weight bands containing both locus-specific and *GFP* sequences are visible in the ZFN-treated GFP<sup>+</sup>-sorted cells, probably owing to targeted integration of head-to-tail vector concatemers in the ZFN site (HT-TI) (**Supplementary Fig. 5**).

### Turning lentiviral vectors into a site-specific integration system

The range of applications of IDLV-ZFN-mediated gene addition would be broadened if the ZFNs targeted a genomic locus chosen for its tolerance to insertion and its permissiveness to transgene expression. Such a system would provide a versatile vehicle for safe and predictable gene delivery.

To investigate this approach, we used ZFNs targeting exon 3 of the chemokine (C-C motif) receptor 5 (*CCR5*) gene, because its homozygous null mutation appears to be well tolerated in humans<sup>42</sup>. We generated two IDLVs for the transient expression of these *CCR5* ZFNs and the cognate donor vector carrying a *GFP* or puromycin-resistance gene (*Puro*<sup>R</sup>) expression cassette flanked by *CCR5* homology arms (**Fig. 5a**). We transduced a panel of cell lines and found high levels of GFP<sup>+</sup> cells in all cell types, although there were significant differences among them (**Fig. 5b** and **Supplementary Fig. 6** online). In K-562 and Jurkat cells, we observed up to 50% GFP<sup>+</sup> cells (K-562: 35 ± 10%, mean ± s.d., *n* = 12; Jurkat: 39 ± 9%, *n* = 7), whereas transduction with donor-IDLV alone resulted in up to 2% GFP<sup>+</sup> cells. PCR analysis showed addition of the *GFP* cassette into the ZFN target site in all cell types tested (**Fig. 5c**) and, in K-562 cells, Southern blot analysis confirmed these data (data not shown). We also found up to 5.4% GFP<sup>+</sup> lymphoblastoid cells (3 ± 1.7%, mean ± s.d., *n* = 8; **Fig. 5d**) after exposure to donor- and ZFN-expressing IDLVs versus a background of 0.1% in cells treated with donor-IDLV alone. Targeted addition into the *CCR5* gene was confirmed by PCR (**Fig. 5e**). When we delivered the *CCR5*-targeting ZFNs with the unrelated *IL2RG* donor by IDLV, we did not observe any increase in GFP expression over the background level obtained with the donor alone (**Fig. 5f**), showing that the enhancement of integration driven by ZFNs requires homologous sequences to the ZFN genomic target

site in the donor vector. We further analyzed a panel of clones isolated from the GFP<sup>+</sup>-treated K-562 cells and found in all cases *GFP* integration into the *CCR5* locus by a mechanism consistent with HDR (**Supplementary Fig. 7** online). As found with the *IL2RG* targeting system (**Supplementary Fig. 5**), the *GFP* cassette was present either as a single copy or in the form of a head-to-tail concatemer with intervening vector sequences of increasing size.

Overall, these studies showed that an IDLV-ZFN system can mediate highly efficient and specific gene addition to a predetermined site in the genome, prompting us to test the approach with primary human stem cells.

### Targeted gene addition in human stem cells

We treated cord blood CD34<sup>+</sup> hematopoietic progenitor cells with donor-IDLVs designed to deliver *GFP* or *Puro*<sup>R</sup> either alone or together with increasing doses of the *CCR5*-targeting ZFN-IDLVs, and measured GFP expression in cells grown in liquid culture and *Puro*<sup>R</sup> in colony-forming cell assays (**Fig. 6a**). Whereas only 0.005% GFP<sup>+</sup> cells and no *Puro*<sup>R</sup> colonies were observed in cultures treated with donor alone, an increasing proportion of cells expressing either marker was found in cultures also exposed to increasing doses of ZFN-expressing IDLVs (up to 0.11% GFP<sup>+</sup>, 0.06 ± 0.02%, mean ± s.d., *n* = 7 experiments with different donors). DNA analysis of the puromycin-resistant colonies, both of erythroid and myeloid origin, showed addition of the *GFP* cassette into the *CCR5* locus in 80% and 90% of the colony-forming cells analyzed, respectively, in two independent experiments (**Fig. 6b**).

Finally, we treated two human ES cell lines (HUES-3 and HUES-1)<sup>43</sup> with the *CCR5*-targeting system and found up to 5.3% GFP<sup>+</sup> cells after treatment with donor- and ZFN-expressing IDLVs (3.5 ± 1.1%,

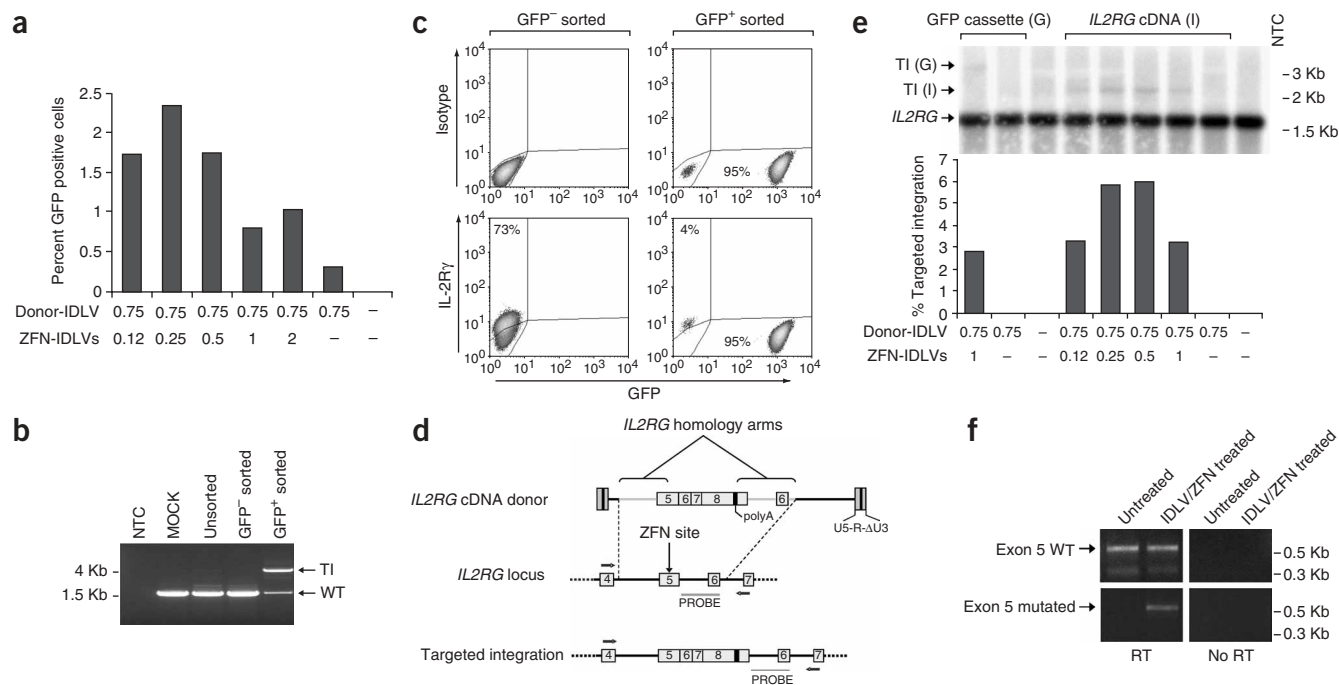


**Figure 4** Targeted gene addition into the *IL2RG* locus in human lymphoblastoid cells. **(a)** Cells were treated with the indicated doses of donor- and ZFN-IDLVs (see **Fig. 3a** for schematics) and analyzed by FACS for GFP expression 15 d after transduction. Data shown are representative of three independent experiments. **(b)** The cells were sorted according to GFP expression and analyzed by PCR and Southern blot (data not shown) to determine targeted integration (TI) of the *GFP* cassette into the *IL2RG* locus. WT: the unmodified *IL2RG* locus. NTC: no template control. **(c)** IL-2R $\gamma$  expression was determined by FACS in sorted cells from **b**. The lower right density dot plot shows that all GFP-positive cells lost expression of the  $\gamma$ -chain, consistent with knock-in of the PGK-*GFP* cassette (approximately one copy of *GFP* DNA per cell as measured by Q-PCR; data not shown) into the sole copy of *IL2RG* in these male cells. **(d)** Top: schematic of the *IL2RG* cDNA donor construct, in which a promoterless, partial *IL2RG* cDNA is flanked by sequences homologous to the ZFN target site. Middle: schematic of the endogenous *IL2RG* locus. Bottom: schematic of targeted gene addition mediated by HDR, leading to knock-in of the cDNA such that expression of this new sequence is driven from the endogenous promoter. PCR primers and probe used in the analysis are indicated. **(e)** Lymphoblastoid cells were treated with the indicated IDLV doses, analyzed by semiquantitative PCR as in **b**, and the results visualized by Southern blot. The amplification products representative of targeted integration of the *GFP* cassette [TI (G)] or the *IL2RG* cDNA [TI (I)] are indicated. The histogram shows the targeted integration levels at the *IL2RG* locus. Note that the percentage of GFP<sup>+</sup> cells in the left-most (G) sample was 2% by FACS, consistent with the molecular analysis. **(f)** Expression of the integrated construct in the treated cells from **e**—0.5  $\mu$ g p24 ZFN-IDLVs sample—was verified by RT-PCR using primers specific for the wild-type or the donor-encoded exon 5 sequence, which carried silent mutations. A control omitting reverse transcriptase (no RT) is shown on the right panels.

mean  $\pm$  s.d.,  $n = 9$ ; **Fig. 6c** and **Supplementary Fig. 8** online), versus 0.3% GFP<sup>+</sup> cells after treatment with donor-IDLV alone. Serial FACS analysis for 1 month showed maintenance of GFP marking (**Fig. 6d**), with GFP<sup>+</sup> colonies expressing the stem cell marker Oct-3/4 (**Fig. 6e**). Targeted *GFP* integration into the *CCR5* locus was shown by PCR in both HUES cultures (**Fig. 6f**). Using PCR and a mismatch-selective endonuclease assay, we determined that up to 28% of the *CCR5* alleles in the HUES cells treated with ZFN-expressing IDLVs carried mutations at the ZFN target site ( $12.7 \pm 6.4\%$ , mean  $\pm$  s.d.,  $n = 11$ , **Fig. 6g**). This is the expected result of NHEJ at the ds break induced by ZFNs and indicates the potential of our strategy to accomplish gene disruption in ES cells. We then derived neural progenitors from the treated HUES cultures and showed maintenance of the newly added *GFP* cassette at the *CCR5* site by PCR (**Fig. 6h**), and its expression in the derived neurons by confocal fluorescence microscopy (**Fig. 6i**).

These data demonstrate that the IDLV-ZFN approach allows gene targeting in human ES cells to previously unattained levels<sup>3,4</sup>, resulting in stable transgene expression without apparent detriment to the self-renewal and neuronal differentiation capacity of the modified cells.

## DISCUSSION

We show here that IDLVs support functional delivery of both ZFNs and donor DNA templates to a variety of human cell types, including hematopoietic progenitors and ES cells. This permits a transient nonintegrating delivery system to yield permanent and heritable genome modification in a site-specific and homology-directed fashion. Three genetically distinct outcomes occur during the repair of the ZFN-induced ds break, namely, gene disruption (**Figs. 2c, 4c** and **6g**), gene correction and/or conversion (**Supplementary Fig. 2, Figs. 1** and **2**) and targeted transgene addition (**Supplementary Fig. 4** and **Figs. 3–6**). Whereas gene disruption results from NHEJ of the recessed strands at the ds break, gene conversion and targeted gene addition likely occur by HDR of the ds break when an exogenous donor sequence is used as a template. According to the design of the latter molecule—that is, whether or not it contains an intervening sequence within the homology to the ZFN-targeted region—either outcome can be specified. Application of the approaches described here allows cells with the desired genotype to be rapidly isolated.

Site-specific viral integration for the permanent, yet safe, modification of the genome has been a long-standing goal of the field. Attempts to retarget the retroviral integrase, however, have been

challenging<sup>44–46</sup>. Here we exploited a catalytically inactive HIV integrase to induce transient accumulation of episomal DNA in the nucleus. This DNA is competent both for transient ZFN expression and as a substrate for homologous recombination and can induce site-specific editing of the genome by HDR of the ZFN-induced ds break. IDLVs can also be designed to be a substrate for the phage  $\phi$ C31 integrase (A.L., M.C. Calos and L.N., unpublished data), suggesting that they can be used in combination with other delivery strategies, including other vector types, to transiently assemble site-specific integration machineries in target cells. In principle, IDLVs may be complemented in *trans* by an active integrase of similar specificity<sup>47</sup>. Whereas this is unlikely to occur in non HIV-infected cells, incorporation of *cis*-acting mutations in the integrase attachment sites of the vector could prevent such a rescue<sup>36</sup>.

An important feature of IDLV gene transfer is the low background integration, which enables a 10- to 100-fold increase in site-specific integration when ZFNs are codelivered. Whereas most integration

events at the ZFN target site appear to be consistent with synthesis-dependent strand annealing<sup>32,48</sup> at both sides of the homologous sequence in the donor vector, a fraction of integrations may occur by engagement of only one homology arm and by NHEJ at the other side (Supplementary Fig. 7). Both the ZFNs and the cognate homologous sequence in the donor DNA drive the high specificity of the process. Use of either ZFNs targeting a control locus or non-homologous donor DNA did not increase integration.

In principle, by modifying the ZFN binding specificity and selecting an appropriate donor sequence, one could target the IDLV-ZFN system to any individual site in the human genome<sup>24,28</sup>. Here we present data obtained targeting two loci. To show gene conversion, we targeted *IL2RG*, whose mutational inactivation causes X-SCID. To demonstrate a site-specific integrating system of potential general applicability, we targeted *CCR5*. In this regard, it will be important to define the features qualifying a locus as a ‘safe harbor’ for transgenesis. Given recent findings that the genome is pervasively

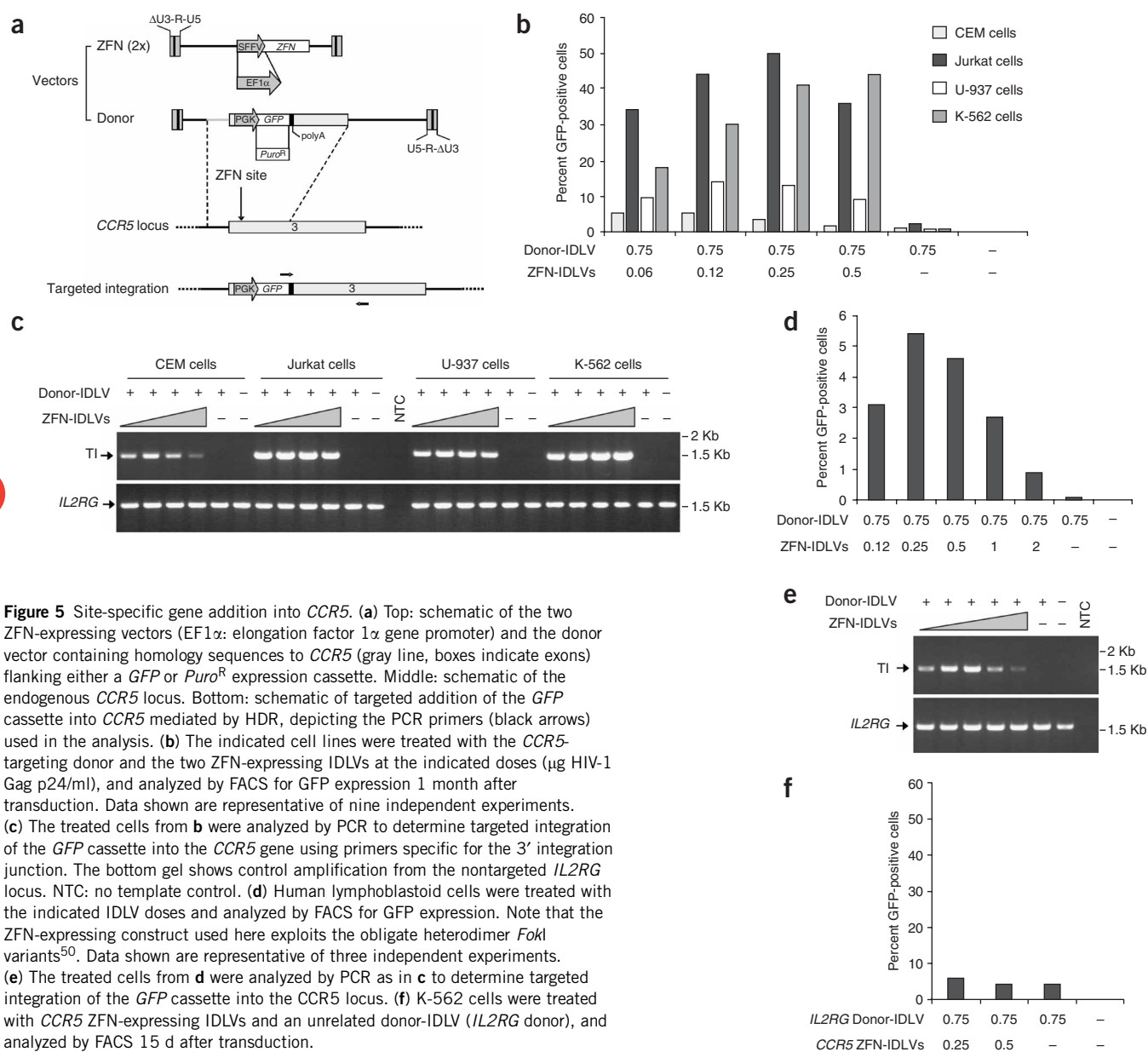


**Figure 5** Site-specific gene addition into *CCR5*. **(a)** Top: schematic of the two ZFN-expressing vectors (EF1 $\alpha$ : elongation factor 1 $\alpha$  gene promoter) and the donor vector containing homology sequences to *CCR5* (gray line, boxes indicate exons) flanking either a *GFP* or *Puro<sup>R</sup>* expression cassette. Middle: schematic of the endogenous *CCR5* locus. Bottom: schematic of targeted addition of the *GFP* cassette into *CCR5* mediated by HDR, depicting the PCR primers (black arrows) used in the analysis. **(b)** The indicated cell lines were treated with the *CCR5*-targeting donor and the two ZFN-expressing IDLVs at the indicated doses ( $\mu$ g HIV-1 Gag p24/ml), and analyzed by FACS for GFP expression 1 month after transduction. Data shown are representative of nine independent experiments. **(c)** The treated cells from **b** were analyzed by PCR to determine targeted integration of the *GFP* cassette into the *CCR5* gene using primers specific for the 3' integration junction. The bottom gel shows control amplification from the nontargeted *IL2RG* locus. NTC: no template control. **(d)** Human lymphoblastoid cells were treated with the indicated IDLV doses and analyzed by FACS for GFP expression. Note that the ZFN-expressing construct used here exploits the obligate heterodimer *FokI* variants<sup>50</sup>. Data shown are representative of three independent experiments. **(e)** The treated cells from **d** were analyzed by PCR as in **c** to determine targeted integration of the *GFP* cassette into the *CCR5* locus. **(f)** K-562 cells were treated with *CCR5* ZFN-expressing IDLVs and an unrelated donor-IDLV (*IL2RG* donor), and analyzed by FACS 15 d after transduction.

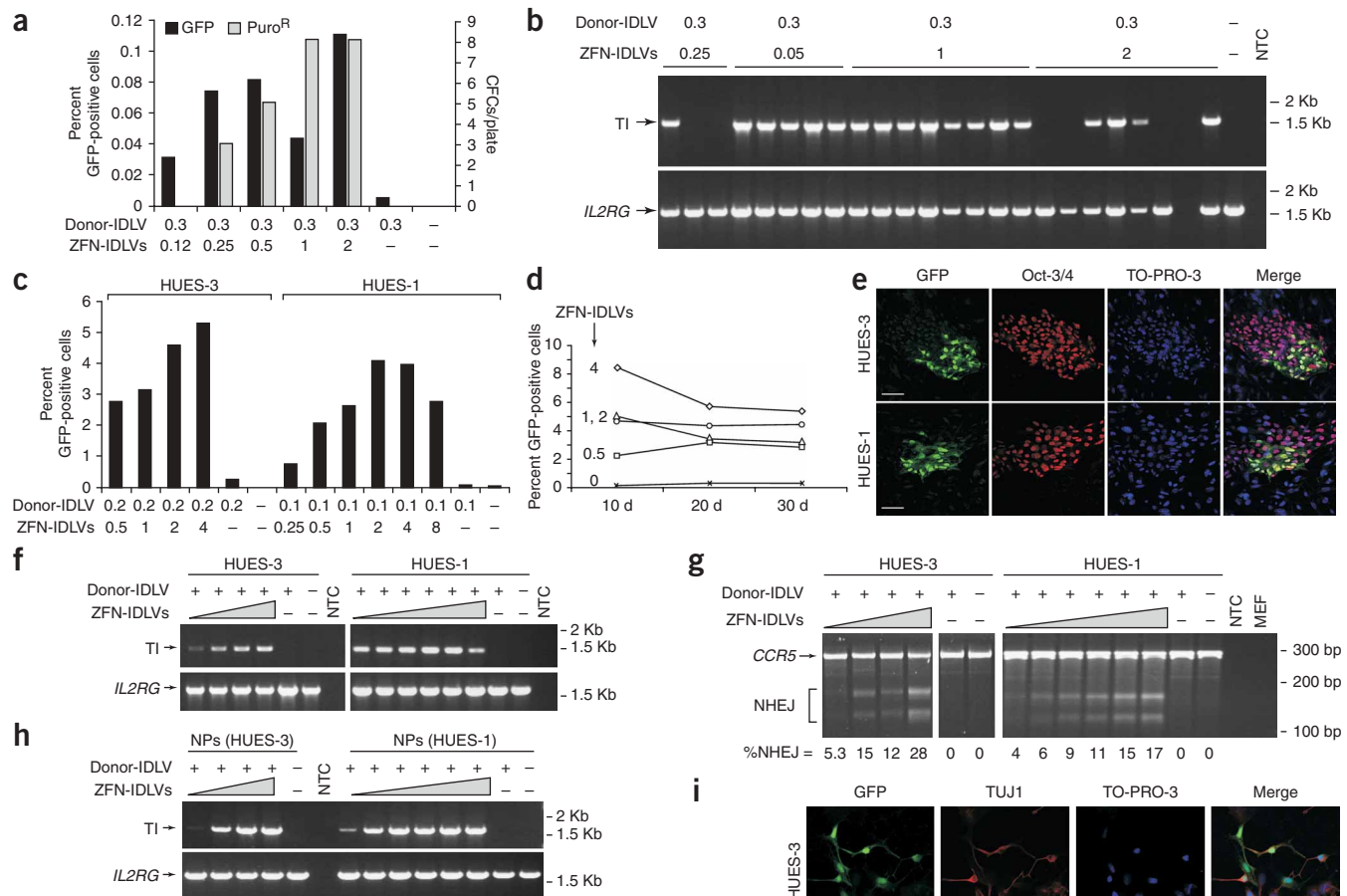


**Figure 6** Targeted gene addition in human stem cells. **(a)** Cord blood CD34<sup>+</sup> progenitor cells were treated with the indicated doses of *CCR5*-targeting donor-IDLV, encoding either GFP or Puro<sup>R</sup>, and *CCR5* ZFN-expressing IDLVs. The histogram shows the percentage of GFP<sup>+</sup> cells in liquid culture measured by FACS 15 d post-transduction (left axis), and of Puro<sup>R</sup> colonies (right axis) in colony-forming cell assays. Data are representative of five and two independent experiments for GFP and Puro<sup>R</sup>, respectively. **(b)** Genomic DNA from Puro<sup>R</sup> colonies was analyzed by PCR for targeted integration of the GFP cassette into the *CCR5* locus. The bottom gel shows control amplification from the nontargeted *IL2RG* locus. NTC, no template control. The control, untreated CFC was obtained from a plate without puromycin. **(c)** HUES-3 and HUES-1 embryonic stem cells were treated with the indicated doses of *CCR5*-targeting GFP donor and ZFN-expressing IDLVs, and analyzed by FACS (**Supplementary Fig. 8**). Note that the EF1 $\alpha$  promoter was used to express ZFNs in HUES cells. Representative experiment of four performed is shown. **(d)** IDLV-treated HUES-3 cells as in **c** were monitored by FACS for GFP expression on the indicated days. **(e)** Representative confocal analysis of HUES cells 2 months post-transduction for GFP (green), the transcription factor Oct-3/4 (red) and nuclear DNA (TO-PRO-3, blue), showing the typical appearance of stem cell colonies containing GFP-positive cells. Scale bar, 120  $\mu$ m. **(f)** PCR performed as in **b** on DNA extracted from treated HUES cultures proved GFP integration into the *CCR5* ZFN target site. **(g)** Mismatch-sensitive endonuclease assay performed on the same DNA as in **f** showed up to 28% mutant *CCR5* alleles upon treatment of the cells with the ZFN-IDLVs. The IDLV-treated cells shown in **c** were differentiated into neurons and analyzed by PCR **(h)** for the maintenance of the added gene into the *CCR5* locus (NP, neural progenitors) and by confocal microscopy **(i)** for the presence of GFP (green) and neuronal class III  $\beta$ -tubulin (TUJ-1, red) double-positive neurons. Nuclear DNA is in blue (TO-PRO-3). Scale bars, 27  $\mu$ m.

transcribed<sup>49</sup>, it may be difficult to select a priori a site that is not undergoing transcription, and, even if there is no evidence of protein-coding activity, it may be equally difficult to rule out involvement in regulatory activity. Alternatively, loci validated by mouse transgenesis, such as Gt(ROSA)26Sor, could be explored. The developmental expression pattern and chromatin status of a locus may influence ZFN accessibility, permissiveness to HDR and maintenance of transgene expression in different types of cells. Moreover, because both HDR and NHEJ can resolve a ZFN-induced ds break, tolerability of mono- and bi-allelic disruption of the target locus must be considered.

Whereas IDLV delivery of ZFNs was well tolerated in our experiments, the application of these reagents in gene and cell therapies will require a thorough safety assessment, including any potential off-target ZFN action. This will comprise determining the number and location of ZFN-induced ds breaks in target cells and evaluating the long-term repopulation and differentiation potential of ZFN-treated stem cells. In this regard we report here that an obligate heterodimerization variant of the *FokI* nuclease domain that reduces the potential for ZFN cleavage at off-target sites mediated by homodimerization of either ZFN<sup>50</sup> remains competent to drive high levels of gene modification.

The efficiency of IDLV-ZFN-mediated gene addition varied significantly among the different cell types tested, with hematopoietic progenitors showing the lowest efficiency. However, even with these cells we could obtain much higher levels of homologous recombination-mediated gene targeting than previously reported in the literature<sup>3</sup>. One rate-limiting factor may be the permissiveness of the target cell to multiple lentiviral infection, known to be much lower in hematopoietic progenitors than in immortalized lymphocytes<sup>51</sup>. Conceivably, use of a single construct to express ZFNs and deliver donor DNA might enhance the efficiency of gene correction or addition even in less permissive cells.

Our findings broaden the application of ZFNs from our earlier demonstration of gene correction of point mutations<sup>33</sup>. Gene correction can now be applied to clinically relevant target cells and extended to the rescue of most mutations occurring at the selected gene, including deletions, using the same pair of ZFNs to knock-in a functional cDNA downstream of the endogenous promoter. X-SCID represents an ideal model for testing our approach<sup>14</sup> as correction of only a small fraction of treated cells, given their strong growth advantage, should allow expansion and restoration of T-cell function *in vivo*. Moreover, by targeting transgenes to an investigator-selected chromosomal site, it will be possible to increase the safety of gene replacement, obtain predictable levels of transgene expression and exploit endogenous promoters to drive transgene expression. The combination of IDLV and ZFNs demonstrated here should enable rapid site-specific editing of the genome in human stem cells, opening new avenues in experimental biology, biotechnology and medicine.

## METHODS

**Vectors.** ZFN-expressing and donor transfer constructs were generated from the HIV-derived self-inactivating transfer construct pCCLsin.cPPT.hPGK.eGFP.Wpre (Supplementary Methods online). The integrase-defective third-generation packaging plasmid pMD.Lg/pRRE.D64VInt was generated by replacing the *BclI*-*AflIII* fragment from plasmid pCMVΔR9-D64V<sup>34</sup>. IDLV stocks were prepared as described<sup>52</sup>. Briefly, 293T cells were cotransfected by calcium phosphate precipitation with the required transfer vector plasmid, the pMD.Lg/pRRE.D64VInt packaging plasmid, the pMD2.VSV-G envelope-encoding plasmid, and pRSV-Rev in the following amounts: 32/12.5/9/6.25 μg DNA per 15-cm dish, respectively. For donor vector production, 1 mM sodium butyrate was added to the collection medium. Vector particles were concentrated 250-fold by ultracentrifugation and measured by HIV-1 Gag p24 immunocapture (Perkin Elmer). Yield ranged from 20 to 200 μg p24/ml, depending on the vector type.

**Zinc finger nucleases.** ZFNs targeting exon 5 of the *IL2RG* gene were previously described<sup>33</sup>. Two sets of *CCR5*-targeting ZFNs were used with either a wild-type or obligate heterodimer *FokI* domain, both targeting exon 3 of the human *CCR5* gene (target gene; ZFP name; target sequence; recognition α-helices): *CCR5*; ZFN-R; AAAGTCAAAG; RSDNLSV, QKINLQV, RSDVLS, QRNHRTT and *CCR5*; ZFN-L; GATGAGGATGAC; DRSNLSR, ISSNLSN, RSDNLAR, TSGNLTR. The obligate heterodimer *FokI* domains generate an active nuclease only by heterodimerization and when incorporated into ZFNs induce ds break with higher specificity<sup>50</sup>. The complete sequence in FASTA format of the *CCR5*-targeting ZFNs is included in Supplementary Figure 9 online. The generation and characterization of these *CCR5*-targeting ZFNs will be described in detail elsewhere (E. Perez, C. June, P.D.G., M.C.H., F.D.U., K.A.K., D.A. and Y.-L., unpublished data).

**Cells and transduction.** Human Epstein-Barr virus-immortalized B lymphocytes, Jurkat, CEM and U-937 cells were maintained in RPMI-1640 (Cambrex); K-562, Mouse Embryonic Fibroblast (MEF), 293T and HEK293 reporter cells in IMDM (Sigma); all media were supplemented with 10% FBS, glutamine and antibiotics. Cells were co-infected at  $1 \times 10^6$  cells/ml with the indicated doses of IDLVs (all vector types added together) for 12–24 h, and then expanded for

analysis. Clones were obtained by limiting dilution. CD34<sup>+</sup> cells were obtained from human cord blood after informed consent according to the Declaration of Helsinki and upon approval by the H. San Raffaele Bioethical Committee. We maintained  $1\text{--}3 \times 10^6$  CD34<sup>+</sup> cells/ml in serum-free StemSpan medium supplemented with early-acting cytokines and incubated with IDLVs in the presence of 0.7 μM proteasome inhibitor MG132 (Calbiochem) for 24 h as described<sup>51</sup>. Cells were then washed and either grown in liquid culture in IMDM 10% FBS plus IL3/IL6/SCF or plated in semi-solid medium in the absence ( $1 \times 10^3$  cells/ml) or presence ( $5 \times 10^5$  cells/ml) of 1 μg/ml puromycin. Human embryonic stem cells (HUES-1 and HUES-3) were grown in KO DMEM supplemented with b-FGF, human albumin, serum replacement, β-mercaptoethanol, glutamine and antibiotics on mitomycin-C treated MEF as described<sup>45</sup>. We infected  $2\text{--}7 \times 10^4$  cells with IDLVs 12 h after plating for 24 h, washed and split every 5 d. HUES differentiation was performed as described in Supplementary Methods. HUES cell work was approved by the Ethical Committee of the Reproductive Technologies Laboratory.

**Flow cytometry.** Infected cells were grown for at least 14 d before FACS (FACSCalibur; Becton Dickinson Pharmingen) to avoid scoring GFP expression from unintegrated vector. For immunophenotypic analysis, the following antibodies were used according to the manufacturer's instruction: phycoerythrin (PE)-conjugated anti-human CD132 (IL-2Rγ; Becton Dickinson Pharmingen), allophycocyanin (APC)-conjugated anti-human LNGFR (Miltenyi Biotec) and PE-conjugated anti-human/mouse SSEA-4 (R&D Systems). Fluorochrome- and dose-matched isotypes were used as controls. 7-Aminoactinomycin D (7-AAD) positive, nonviable cells were excluded from the analysis, and  $1\text{--}5 \times 10^5$  viable cells were scored per analysis. Analysis was performed using CellQuest (Becton Dickinson Pharmingen) or WindMDI software.

**Gene conversion and targeted integration analysis.** Genomic DNA was isolated with either Blood & Cell Culture DNA Midi Kit or DNeasy Tissue Kit (QIAGEN). To measure editing of the *IL2RG* gene we modified a previously described protocol<sup>33</sup>. Briefly, 100 ng genomic DNA was subjected to PCR (PCR SuperMix High Fidelity, Invitrogen) using primers and conditions indicated in Supplementary Methods. PCR products were purified with MicroSpin G-50 Columns (Amersham Biosciences) and digested with the indicated enzymes overnight. Digested DNA was purified, separated on 1% agarose, transferred to nylon membrane (Hybond-N+, Amersham Biosciences) and probed with the indicated <sup>32</sup>P-radiolabeled sequence. Membranes were exposed in a Storage Phosphor Screen, and Typhoon 9410 densitometric scanning (Amersham Biosciences) was used to quantify band intensity using the ImageQuant TL software. Editing efficiencies were calculated as: [intensity of the edited band / (intensity of the wild-type + edited bands)] × 100. To detect targeted integration in the *IL2RG* gene or the *CCR5* gene, we subjected 40–200 ng genomic DNA to PCR with a combination of AmpliTaq Gold (Applied Biosystems) and TaqExtender PCR Additive (Stratagene) using primers and conditions indicated in Supplementary Methods. For mRNA analysis, 2 μg total RNA extracted from  $8 \times 10^6$  cells using Tri Reagent (Sigma) were reverse transcribed using oligo(dT)<sub>20</sub> according to SuperScript III First-Strand Synthesis System (Invitrogen). A fraction of the resulting cDNA was amplified by PCR using primers designed to discriminate between wild-type and mutated exon 5 (Supplementary Methods). PCR amplicons were resolved on agarose gel and visualized by ethidium bromide staining. For Southern blot analyses, genomic DNA was digested with the indicated enzymes and purified. Matched DNA amounts were separated on 0.8% agarose, transferred to a nylon membrane and probed with the indicated <sup>32</sup>P-radiolabeled sequences. Densitometric analysis was performed as before. For Q-PCR, 200 ng genomic DNA was analyzed using primers and probes complementary to the vector backbone sequence (RRE), the GFP sequence, the ΔLNGFR sequence and human *TERT*, the latter amplification used as normalizer, as previously described<sup>51,53</sup>. To detect ZFN IDLVs, we used primers and probe complementary to the *FokI* sequence (Supplementary Methods). Standard curves for RRE and GFP were generated by serial dilutions of DNA from human cell lines containing a known number of vector integrations, whereas for ΔLNGFR and ZFN amplification, DNA from untreated cells was mixed with known amounts of ΔLNGFR and ZFN plasmids.



**Requests for materials.** mholmes@sangamo.com for ZFN reagents and naldini.luigi@hsr.it for IDLV reagents.

*Note: Supplementary information is available on the Nature Biotechnology website.*

#### ACKNOWLEDGMENTS

We are grateful to Lucia Sergi Sergi and Anna Zingale for technical help, Giovanna Lazzari for advice with HUES cultures, Rosa Bacchetta and Alessandro Aiuti for providing lymphoblastoid cells, Brian Brown and Bernhard Gentner for helpful discussion. We also thank Russell DeKelver, Jianbin Wang, Aleida Perez and Anna Lam for donor DNA construct generation, Jeffrey Miller, Victor Bartsevich, Dmitry Guschin, Igor Rupniewski, Yanhong Kong, Edward Rebar, Lei Zhang, Adam Waite, Deng Xia, Sarah Hinkley and members of the Sangamo production group for the design and generation of the ZFNs used in this study, and Sean Brennan for reading the manuscript. Research was supported by grants from Telethon (TIGET), National Institutes of Health (2 P01 HL053750-11 CFDA No. 93.839), EU (CONCERT, LSHB-CT-2004-005242) and Sangamo BioSciences to L.N., and European Science Foundation (EUROCORES Programme, EuroSTELLS) to C.G. HUES were kindly provided by D. Melton from Harvard Stem Cell Institute, under specific Materials Transfer Agreement to C.G.

#### AUTHORS CONTRIBUTIONS

A.L. designed, performed experiments and wrote the paper; P.G., C.M.B., Y.-L.L. and K.A.K. performed experiments; S.C. performed ES cell cultures; D.A. and F.D.U. designed experiments; C.G. coordinated ES cell work; P.D.G. and M.C.H. designed experiments and wrote the paper; and L.N. coordinated the project, designed experiments and wrote the paper.

#### COMPETING INTERESTS STATEMENT

The authors declare competing financial interests: details accompany the full-text HTML version of the paper at <http://www.nature.com/naturebiotechnology/>.

Published online at <http://www.nature.com/naturebiotechnology/>

Reprints and permissions information is available online at <http://ngp.nature.com/reprintsandpermissions>

1. Capecchi, M.R. Generating mice with targeted mutations. *Nat. Med.* **7**, 1086–1090 (2001).
2. Chen, J.M., Cooper, D.N., Chuzhanova, N., Ferec, C. & Patrinos, G.P. Gene conversion: mechanisms, evolution and human disease. *Nat. Rev. Genet.* **8**, 762–775 (2007).
3. Hatada, S., Nikkuni, K., Bentley, S.A., Kirby, S. & Smithies, O. Gene correction in hematopoietic progenitor cells by homologous recombination. *Proc. Natl. Acad. Sci. USA* **97**, 13807–13811 (2000).
4. Zwaka, T.P. & Thomson, J.A. Homologous recombination in human embryonic stem cells. *Nat. Biotechnol.* **21**, 319–321 (2003).
5. Evans, M.J. The cultural mouse. *Nat. Med.* **7**, 1081–1083 (2001).
6. Smithies, O. Forty years with homologous recombination. *Nat. Med.* **7**, 1083–1086 (2001).
7. Hendrie, P.C. & Russell, D.W. Gene targeting with viral vectors. *Mol. Ther.* **12**, 9–17 (2005).
8. Baum, C. *et al.* Chance or necessity? Insertional mutagenesis in gene therapy and its consequences. *Mol. Ther.* **9**, 5–13 (2004).
9. Bushman, F. *et al.* Genome-wide analysis of retroviral DNA integration. *Nat. Rev. Microbiol.* **3**, 848–858 (2005).
10. Montini, E. *et al.* Hematopoietic stem cell gene transfer in a tumor-prone mouse model uncovers low genotoxicity of lentiviral vector integration. *Nat. Biotechnol.* **24**, 687–696 (2006).
11. Nienhuis, A.W., Dunbar, C.E. & Sorrentino, B.P. Genotoxicity of retroviral integration in hematopoietic cells. *Mol. Ther.* **13**, 1031–1049 (2006).
12. Aiuti, A. *et al.* Correction of ADA-SCID by stem cell gene therapy combined with nonmyeloablative conditioning. *Science* **296**, 2410–2413 (2002).
13. Gaspar, H.B. *et al.* Gene therapy of X-linked severe combined immunodeficiency by use of a pseudotyped gammaretroviral vector. *Lancet* **364**, 2181–2187 (2004).
14. Cavazzana-Calvo, M., Lagresle, C., Hacein-Bey-Abina, S. & Fischer, A. Gene therapy for severe combined immunodeficiency. *Annu. Rev. Med.* **56**, 585–602 (2005).
15. Ott, M.G. *et al.* Correction of X-linked chronic granulomatous disease by gene therapy, augmented by insertional activation of MDS1–EVI1, PRDM16 or SETBP1. *Nat. Med.* **12**, 401–409 (2006).
16. Hacein-Bey-Abina, S. *et al.* LMO2-associated clonal T cell proliferation in two patients after gene therapy for SCID-X1. *Science* **302**, 415–419 (2003).
17. Woods, N.B., Bottero, V., Schmidt, M., von Kalle, C. & Verma, I.M. Gene therapy: therapeutic gene causing lymphoma. *Nature* **440**, 1123 (2006).
18. Thrasher, A.J. *et al.* Gene therapy: X-SCID transgene leukaemogenicity. *Nature* **443**, E5; discussion E6–7 (2006).
19. Goyenvall, A. *et al.* Rescue of dystrophic muscle through U7 snRNA-mediated exon skipping. *Science* **306**, 1796–1799 (2004).
20. Tahara, M. *et al.* Trans-splicing repair of CD40 ligand deficiency results in naturally regulated correction of a mouse model of hyper-IgM X-linked immunodeficiency. *Nat. Med.* **10**, 835–841 (2004).
21. Chamberlain, J.R. *et al.* Gene targeting in stem cells from individuals with osteogenesis imperfecta. *Science* **303**, 1198–1201 (2004).
22. Miller, D.G. *et al.* Gene targeting *in vivo* by adeno-associated virus vectors. *Nat. Biotechnol.* **24**, 1022–1026 (2006).
23. Calos, M.P. The phiC31 integrase system for gene therapy. *Curr. Gene Ther.* **6**, 633–645 (2006).
24. Porteus, M.H. & Carroll, D. Gene targeting using zinc finger nucleases. *Nat. Biotechnol.* **23**, 967–973 (2005).
25. Porteus, M.H. & Baltimore, D. Chimeric nucleases stimulate gene targeting in human cells. *Science* **300**, 763 (2003).
26. Bibikova, M. *et al.* Stimulation of homologous recombination through targeted cleavage by chimeric nucleases. *Mol. Cell. Biol.* **21**, 289–297 (2001).
27. Miller, J., McLachlan, A.D. & Klug, A. Repetitive zinc-binding domains in the protein transcription factor IIIA from *Xenopus oocytes*. *EMBO J.* **4**, 1609–1614 (1985).
28. Pabo, C.O., Peisach, E. & Grant, R.A. Design and selection of novel Cys2His2 zinc finger proteins. *Annu. Rev. Biochem.* **70**, 313–340 (2001).
29. Tan, S. *et al.* Zinc-finger protein-targeted gene regulation: genomewide single-gene specificity. *Proc. Natl. Acad. Sci. USA* **100**, 11997–12002 (2003).
30. Kim, Y.G., Cha, J. & Chandrasegaran, S. Hybrid restriction enzymes: zinc finger fusions to Fok I cleavage domain. *Proc. Natl. Acad. Sci. USA* **93**, 1156–1160 (1996).
31. Bitinaite, J., Wah, D.A., Aggarwal, A.K. & Schildkraut, I. FokI dimerization is required for DNA cleavage. *Proc. Natl. Acad. Sci. USA* **95**, 10570–10575 (1998).
32. O'Driscoll, M. & Jeggo, P.A. The role of double-strand break repair - insights from human genetics. *Nat. Rev. Genet.* **7**, 45–54 (2006).
33. Urnov, F.D. *et al.* Highly efficient endogenous human gene correction using designed zinc-finger nucleases. *Nature* **435**, 646–651 (2005).
34. Naldini, L. *et al.* In vivo gene delivery and stable transduction of nondividing cells by a lentiviral vector. *Science* **272**, 263–267 (1996).
35. Vargas, J. Jr., Gusella, G.L., Najfeld, V., Klotman, M.E. & Cara, A. Novel integrase-defective lentiviral episomal vectors for gene transfer. *Hum. Gene Ther.* **15**, 361–372 (2004).
36. Nightingale, S.J. *et al.* Transient gene expression by nonintegrating lentiviral vectors. *Mol. Ther.* **13**, 1121–1132 (2006).
37. Yanez-Munoz, R.J. *et al.* Effective gene therapy with nonintegrating lentiviral vectors. *Nat. Med.* **12**, 348–353 (2006).
38. Philippe, S. *et al.* Lentiviral vectors with a defective integrase allow efficient and sustained transgene expression in vitro and in vivo. *Proc. Natl. Acad. Sci. USA* **103**, 17684–17689 (2006).
39. Leavitt, A.D., Robles, G., Alesandro, N. & Varmus, H.E. Human immunodeficiency virus type 1 integrase mutants retain in vitro integrase activity yet fail to integrate viral DNA efficiently during infection. *J. Virol.* **70**, 721–728 (1996).
40. Elliott, B., Richardson, C., Winderbaum, J., Nickoloff, J.A. & Jasin, M. Gene conversion tracts from double-strand break repair in mammalian cells. *Mol. Cell. Biol.* **18**, 93–101 (1998).
41. Buckley, R.H. Molecular defects in human severe combined immunodeficiency and approaches to immune reconstitution. *Annu. Rev. Immunol.* **22**, 625–655 (2004).
42. Lim, J.K., Glass, W.G., McDermott, D.H. & Murphy, P.M. CCR5: no longer a “good for nothing” gene—chemokine control of West Nile virus infection. *Trends Immunol.* **27**, 308–312 (2006).
43. Cowan, C.A. *et al.* Derivation of embryonic stem-cell lines from human blastocysts. *N. Engl. J. Med.* **350**, 1353–1356 (2004).
44. Tan, W., Dong, Z., Wilkinson, T.A., Barbas, C.F. III & Chow, S.A. Human immunodeficiency virus type 1 incorporated with fusion proteins consisting of integrase and the designed polydactyl zinc finger protein E2C can bias integration of viral DNA into a predetermined chromosomal region in human cells. *J. Virol.* **80**, 1939–1948 (2006).
45. Bushman, F.D. & Miller, M.D. Tethering human immunodeficiency virus type 1 preintegration complexes to target DNA promotes integration at nearby sites. *J. Virol.* **71**, 458–464 (1997).
46. Ciuffi, A., Diamond, T.L., Hwang, Y., Marshall, H.M. & Bushman, F.D. Modulating target site selection during human immunodeficiency virus DNA integration in vitro with an engineered tethering factor. *Hum. Gene Ther.* **17**, 960–967 (2006).
47. Fletcher, T.M. III *et al.* Complementation of integrase function in HIV-1 virions. *EMBO J.* **16**, 5123–5138 (1997).
48. Sung, P. & Klein, H. Mechanism of homologous recombination: mediators and helicases take on regulatory functions. *Nat. Rev. Mol. Cell Biol.* **7**, 739–750 (2006).
49. Birney, E. *et al.* Identification and analysis of functional elements in 1% of the human genome by the ENCODE pilot project. *Nature* **447**, 799–816 (2007).
50. Miller, J.C. *et al.* An improved zinc-finger nuclease architecture for highly specific genome editing. *Nat. Biotechnol.* **25**, 778–785 (2007).
51. Santoni de Sio, F.R., Cascio, P., Zingale, A., Gasparini, M. & Naldini, L. Proteasome activity restricts lentiviral gene transfer into hematopoietic stem cells and is down-regulated by cytokines that enhance transduction. *Blood* **107**, 4257–4265 (2006).
52. Follenzi, A. & Naldini, L. Generation of HIV-1 derived lentiviral vectors. *Methods Enzymol.* **346**, 454–465 (2002).
53. Brown, B.D., Venneri, M.A., Zingale, A., Sergi Sergi, L. & Naldini, L. Endogenous microRNA regulation suppresses transgene expression in hematopoietic lineages and enables stable gene transfer. *Nat. Med.* **12**, 585–591 (2006).